Experimental study on the effect of bubble cluster shape on cavitation in water hydraulic valve

IOP Conf. Series: Earth and Environmental Science **240** (2019) 062049 doi:10.1088/1755-1315/240/6/062049

Experimental study on the effect of bubble cluster shape on cavitation in water hydraulic valve

H H Wang, H Xu, V Pooneeth, L Y Jiao and M Y Hu

College of Mechanical and Electrical Engineering, Harbin Engineering University, Harbin, China

E-mail: railway_dragon@sohu.com

Abstract. The experimental studies presented in this paper attempt to study the cavitation in water hydraulic valve from the perspective of the bubble cluster shape and its change over time. Based on the 3-D vision method of combining a high-speed camera with 5 plane mirrors, the characteristics of the bubble cluster shape with an opaque object are discussed in a three dimensional approach. By applying the bionic structure at the valve seat which changes the fluid flow performance, the shape features of the bubble cluster, including bubble number, contour and equivalent density in vertical direction, were altered. Taking into consideration the bubble cluster flow pattern and the development process from generation to collapse of the bubble, the degree of cavitation of the constraint space inside the valve was analyzed and estimated. The analysis compared two sets of experiment and testified the efficiency of the bionic jet hole structure on valve seat.

1. Introduction

With growing environmental problems, water hydraulics has become one of the salient fields, regarding the modern hydraulic transmission technologies which is due to almost no pollution, advent of low cost simple systems and so on [1, 2]. Compared to the oil hydraulics system, cavitation has been recurrent in water hydraulic systems owing to the saturated vapor pressure being higher than the static pressure [3]. The occurrence of cavitation has highly been unfavorable in hydraulics machinery which resulted in erosion, noise and vibrations. The foremost cavitation observation was studied by Benjamin and Ellis, using a rotating-drum camera to observe the bubbles in fluid flow [4]. The results showed serious damage to the solid wall owing to the collapsing of bubbles and formation of violent impacts in the liquid near the side wall. Therefore, a better understanding of the flow pattern of cavitation bubbles inside water hydraulic valves is required to estimate the cavitation erosion.

For the last 10 years or so, there has been a trend to use high-speed camera technology to study cavitation bubbles [5, 6]. With regard to the water hydraulics valve, the opaque object in the valve port, i.e. the valve core and the rod, is the typical structure which is an unavoidable problem during cavitation observation. Xue et al. [7] presented a virtual stereo sensor including 4 mirrors to study the flow mechanism in bubbly flows. The images from two sides of the transparent valve could not record all the bubbles around the opaque object. Therefore, based on the experimental method of [7], 5 plane mirrors were optimally arranged to catch the cavitation images from three sides of the valve in this paper.

IOP Conf. Series: Earth and Environmental Science **240** (2019) 062049 doi:10.1088/1755-1315/240/6/062049

2. Experimental setup

2.1. Overall structure

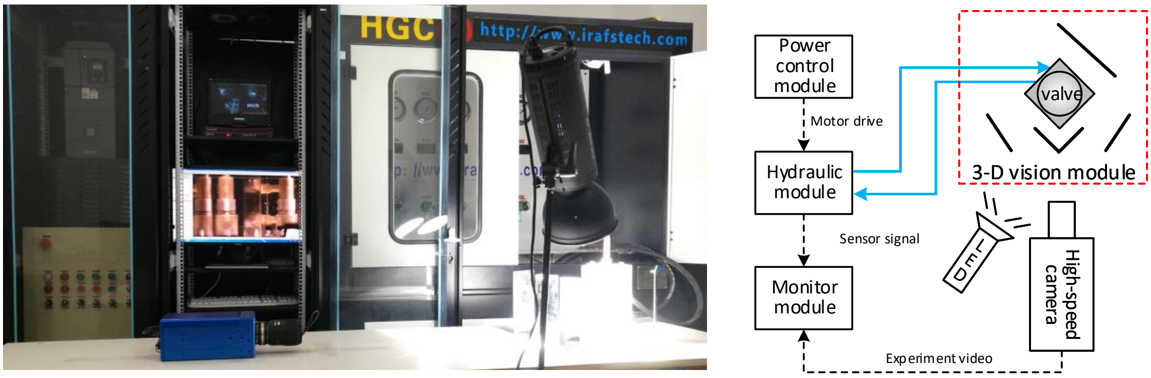

Figure 1. Experimental setup and sketch of the test rig

Figure 1 shows the main test rig used to observe the Virtual 3-D vision and the overall structure of the corresponding modules in the water hydraulics experimental system. The frequency converter in the power control module is used to control the rotation speed of water hydraulic pump, i.e. the inlet pressure of the valve. The hydraulic module consists of the hydraulic pump, pipes, various control valves and sensors. The experimental data including the sensor signal data and experiment videos are collected in an industrial personal computer of the monitor module. In conjunction with LED light, the visualized cavitation module was observed using a high-speed camera. The high speed camera is capable of taking images of 1280×860 pixels at 4000 f/s and uses a 60mm lens.

2.2. 3-D vision module

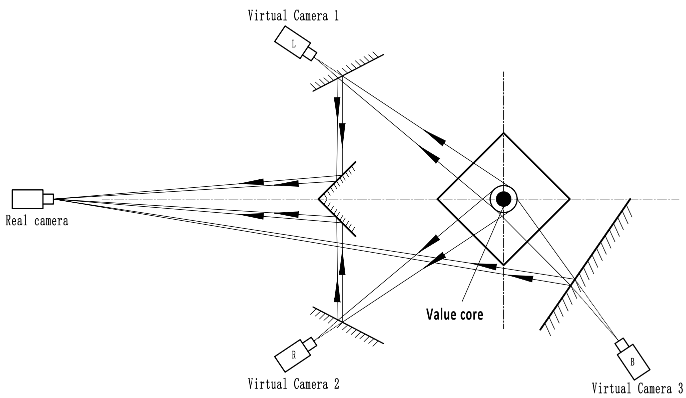

Figure 2. Imaging model of the 3-D vision module

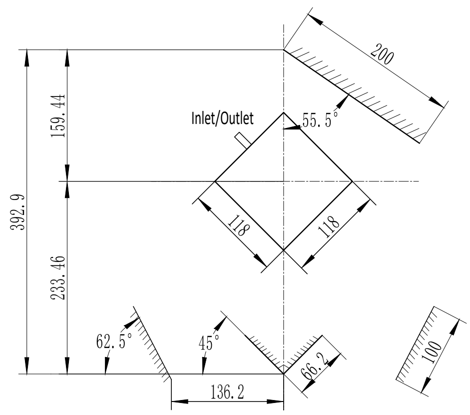

Figure 3. Dimensions of the 3-D vision module

Using a 5 plane mirror optimal arrangement as shown in Figure 3, the image information from the three sides of the transparent valve is taken by a single camera. And the synchronization between the image acquisition and valve position is ensured by using single camera. Owing to the inlet and outlet coupler and the hydraulic hoses interfering with the vision, the image information from the fourth side face is ignored. The virtual cameras 1, 2 and 3 record the left

(L), right (R) and back (B) sides of the valve, respectively. The image from the L, R and B virtual cameras capture all the cavitation bubbles around the valve core. Figure 2 describes the dimensions of the 3-D vision module, including the relative position of the transparent valve and 5 plane mirrors.

2.3. Transparent throttle valve

Poly(methyl methacrylate) (PMMA), a transparent acrylic glass was used to manufacture the valves body. Along with its refractive index (1.490) being relatively closer to the fluid used (water (1.333)) and its ability to withstand higher pressures of 20 bar, PMMA was used to manufacture the throttle valves body. Operating at 20°C, no correction factor was required and high light transmission was observed with no substantial image distortion [8].

Bio-inspired from a shark jetting water out of its gills thus forming a jet flow with significant influence on its flow field, a similar jet hole structure was designed in the valve seat to reduce the cavitation [9]. This aided bionic design can have a positive effect on the pressure distribution and then reduce the flow resistance between the valve core and seat. To test its effectiveness, two valve seats, with and without the bionic structure, as shown in Figure 4, were made to compare the cavitation situation in the water hydraulics throttle valve.

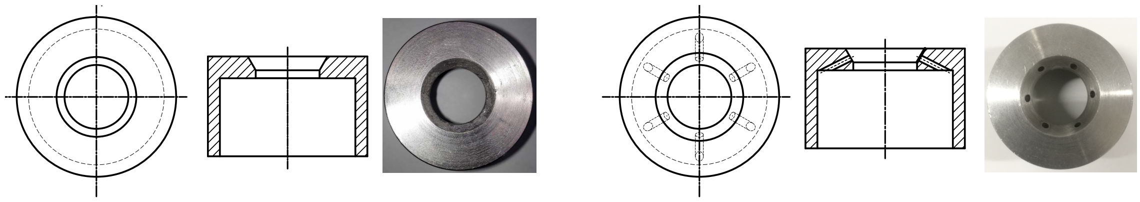

(a) (b)

Figure 4. Two different valve seats

3. Mathematical model and algorithm

3.1. Feature extraction of 2-D bubbles

The result from the virtual stereo vision sensor is a true color video file which contains a group of images. The valve port area where the cavitation bubbles appeared was processed and analyzed. An image processing algorithm based on the frame differencing method was developed for the feature detection of the cavitation bubbles. All the bubble features of the relative motion compared to the previous frame were extracted. As shown in Figure 5, the left, right and back image area were manually extracted into three relative videos, and the 2-D bubble features were detected. The bubble feature parameters, including the coordinates, the width and the height were obtained. To better simulate the shape of cavitation bubbles, an ellipse was applied as the bubble outline. Some larger bubble features could be bubble clusters, including multiple closely packed bubbles. Some smaller bubble features could be the bubbles under developing state or in collapsing mode. In addition, the flow pattern of the bubbles from the left, right, and back sides are clearly illustrated.

3.2. Feature identification of the opaque object

The valve seat and the valve core were made up using stainless steel. The material used for the valve rod was brass. As a result, there was a distinct and stable color difference feature at the interface between the valve core and rod. To build a general 3-D coordinates system, the midpoint of the boundary line between the valve core and the valve rod is defined as the coordinates origin of the 3-D model. The algorithm of the valve core identification is based on

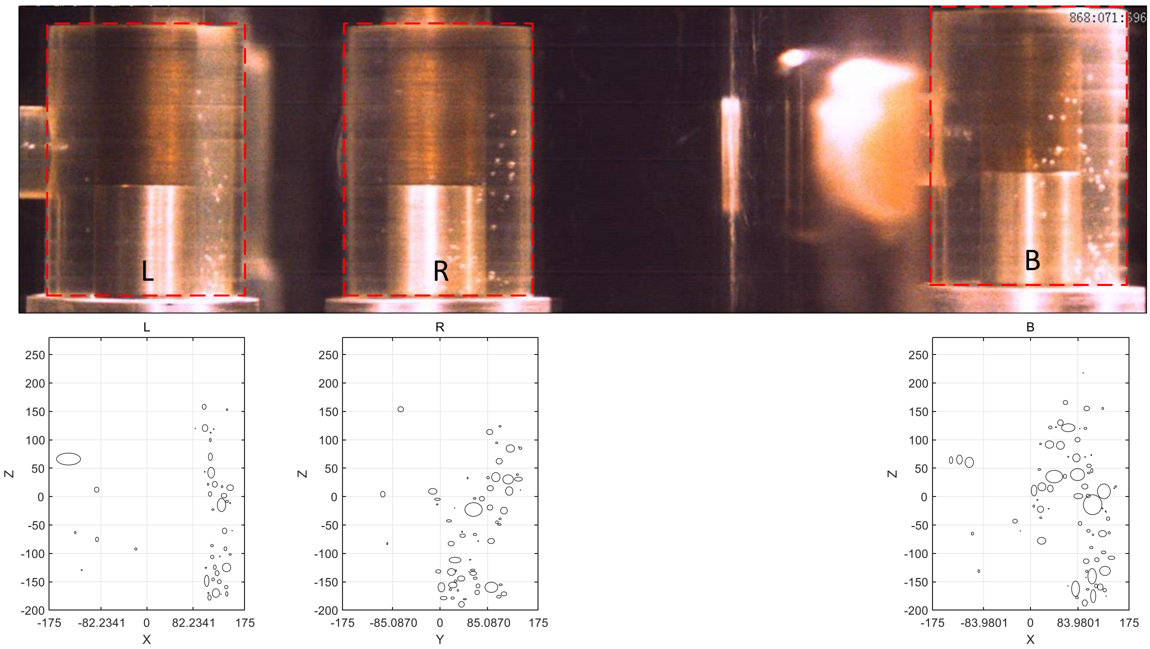

Figure 5. Detection results of the 2-D bubble features

the Faster R-CNN method developed by Ren et al. [10] which is a mainstream deep learning method for object detection. As shown in Figure 6, the object detection model based on deep learning required a larger number of training samples. After processing the training model, the detection accuracy met the adequate requirements. Thus, the coordinates of the object valve core contour were obtained through the Faster R-CNN model. After about 80,000 iterations of the learning process, the algorithm achieved its convergence.

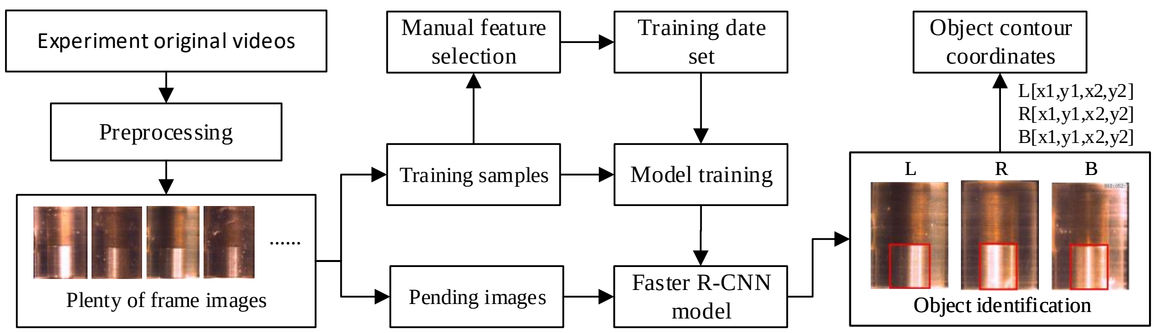

Figure 6. Block diagram of Faster R-CNN model

3.3. 3-D reconstruction of the bubble cluster

The origin of the coordinates is located at the center of the contact surface between the valve core and the rod. As shown in Figure 5, the horizontal and vertical direction of the left side and the back side were defined as the X and Z coordinate axis. Furthermore, the X-axis positive direction of the L plane was the same as the B plane due to the different situations of mirror reflection. The horizontal and vertical direction of the right side were defined as the Y and Z coordinate axis, respectively. As shown in Figure 7, the space of the valve port was divided into

15 parts to reduce the matching scope and error. In the process of the 3-D reconstruction of the bubble cluster, the bubble from different sides were matched with the same bubble in a 3-D space. The R side provided the values of the Y axis to the bubbles from L or B sides. Due of the deficiency of vision from the R side, the y axis of the bubbles belonging to the space of the L2, L1B4 and B3 was defined as a random value. The mathematical model of bubble matching is presented as follows:

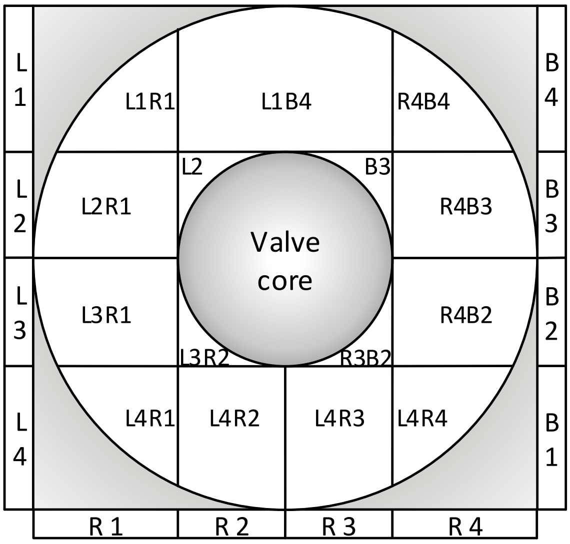

Figure 7. Space partition from the three sides

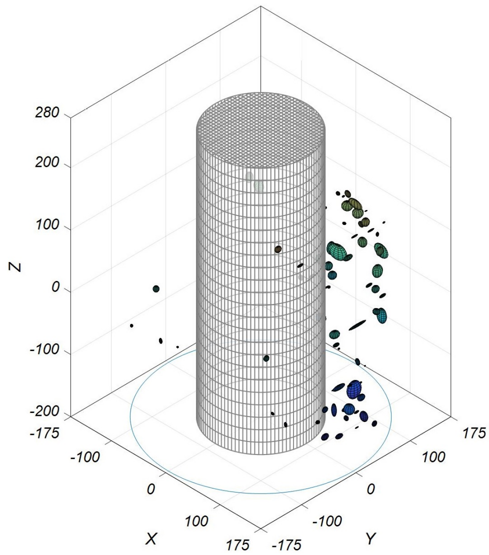

Figure 8. 3-D reconstruction result of bubble cluster

$$D_{ij} = 1 + |z_i - z_j| \tag{1}$$

$$H_{ij} = \frac{a_i}{b_i} + \frac{b_i}{a_i} \tag{2}$$

$$M_{ij} = D_{ij}H_{ij} = \frac{(1 + |z_i - z_j|)(a_i^2 + b_i^2)}{a_i b_i} \tag{3}$$

i and j are two bubbles on different sides. D_{ij} is an index considering the difference of the z axis between the two matching 2-D bubbles. H_{ij} is defined for taking into account the width difference. a_i, b_i, c_i are the three semi-major axis on the x, y, z axes. M_{ij} is the marching index of the comprehensive judgement of D_{ij} and H_{ij}. If M_{ij} is less than the M_{max}, the bubbles marked as i and j are considered as a marching 3-D bubble candidate. After matching all the bubbles from the three sides, the couples with the minimum M_{ij} in their matching candidates are selected as the matched 3-D bubbles. Figure 8 presents the 3-D reconstructed bubble cluster of the images in Figure 5. The shape of an ellipsoid was applied to simulate the bubbles. The results present a vivid bubble cluster shape.

4. Analysis of the experiment results

To testify the efficiency of the bionic structure on reducing cavitation bubbles, two sets of the experiment were performed under the same external conditions. The inlet pressure of the transparent valve was stabilized at 0.5 MPa. The valve seat used in the first experiment had a normal structure whereas the valve seat in the second experiment had a bionic structure with 6 jet holes.

The time interval between the two adjacent frames is converted in Equation 4:

$$\Delta t_f = \frac{\Delta S_f \times 1000}{r_f} \tag{4}$$

The frame rate Δr_f was 3471 per second. The frame step ΔS_f in analysis of the bubble data in Figure 1 was 10. So, $\Delta t_f = 2.881$ ms. After the water flowed through the valve port for a period time and the pressures of the inlet and outlet were stabilized, two sets of experiment videos in the same time consisting of 750 frames were extracted. The total time of the selected range was only about 0.216 s, that reflected the high speed bubble flow and the advantage of the high-speed camera capturing rapidly the changing process of the cavitation bubbles.

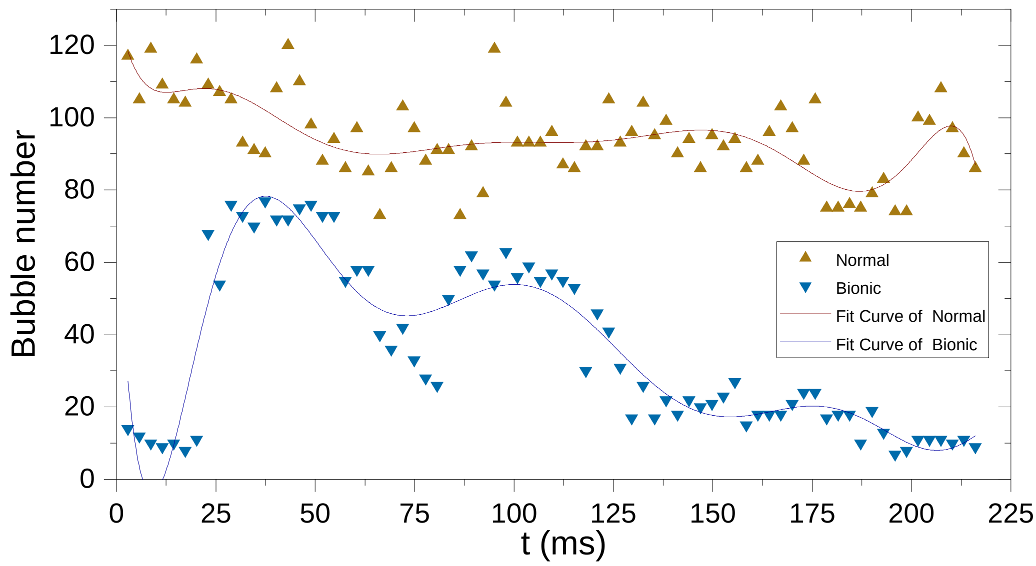

Figure 9. Change of bubble number over time

As shown in Figure 9, the common bubble number of the bionic structure is significantly less than that of normal structure. The bubble number of the normal structure tends to be stable, and the bubble number of the bionic structure firstly rises rapidly and then gradually decreases.

$$P_V = \frac{\sum_{i=1}^{n} \frac{4}{3}\pi a_i b_i c_i}{\pi(R_{fluid} - r_{core})h} \times 100\% \tag{5}$$

The cavitation volume percentage at each frame is stated as Equation 5. R_{fluid} is the radius of the fluid field in the valve. r_{core} is the radius of the valve core. h is the height of the fluid field in the valve. Figure 10 presents the change of the cavitation volume percentage over time. The common cavitation volume percentage of the bionic structure was significantly less than that of normal structure according to the fit curves. Besides, the change of the P_V between the adjacent time points was much greater than that of the bionic structure which indicated that the generation and collapse of the bubble cluster was much serious than that of the bionic structure. Analyzing Figure 10 with Figure 9, there is a positive correlation between the number of bubbles and the percentage of cavitation.

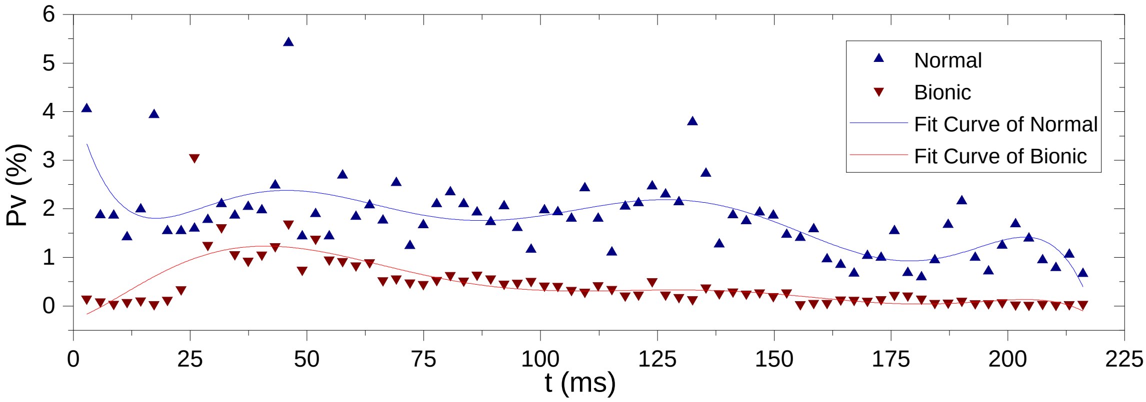

Figure 10. Change of the P_V over time

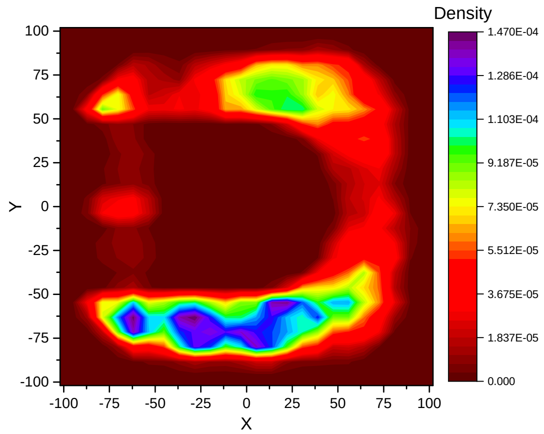

(a) Normal

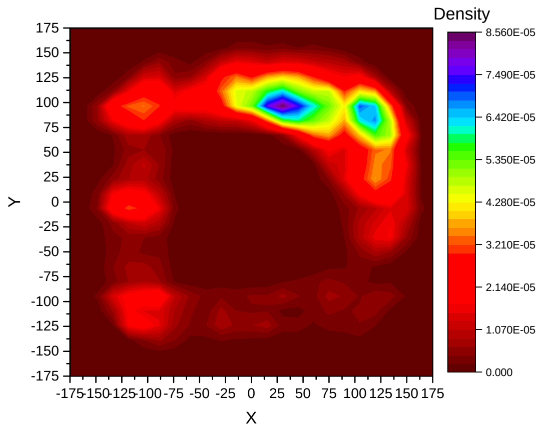

(b) Bionic

Figure 11. Kernel density of the cavitation bubbles on XY plane

The total bubble numbers in the two period videos are 6981 (Normal) and 3018 (Bionic) respectively. Through analysing, the average volume degree of the single bubble is 191.28 (Normal) and 107.14 (Bionic).

Figure 11 shows the bubble density of the two sets of video in the whole time. The cavitation in normal structure is much more serious than that of the bionic structure. And the distribution of the bubble cluster is more dispersive than the bionic one, which means more cavitation erosion. All these analysis states the efficiency of the bionic structure at the valve seat.

5. Conclusion

A 3-D vision method combining a high-speed camera with 5 plane mirrors for studying the cavitation bubble cluster in water hydraulic valves has been described in this paper. Using frame differencing method, the 2-D bubble features were detected from the images obtained from the three sides of the transparent valve. A deep learning algorithm was applied for the object identification of the opacification, i.e. the valve core and the rod. Based on the 2-D bubble coordinates and size and the 3-D coordinates origin, the 3-D bubble cluster in the valve was reconstructed by matching the 2-D bubble features between adjacent sides of the valve. From a comparative analysis of two sets of experiment, the characteristic of the bubble cluster inside the valve was studied and the efficiency of the bionic structure was validated.

IOP Conf. Series: Earth and Environmental Science **240** (2019) 062049 doi:10.1088/1755-1315/240/6/062049

The current research in this paper focuses on the quantitative analysis of the cavitation. However, the cavitation erosion is not only driven by the bubble quantity but the implosion place too, which will be our future research interest.

Acknowledgment

This paper is funded by the International Exchange Program of Harbin Engineering University for Innovation-oriented Talents Cultivation. This work was supported by the Natural Science Foundation of the Heilongjiang Province of China under Grant F2016003 and Validation System for Test under Grant (KY10700150064).

References

[1] Singh R, Tiwari S K and Mishra S K 2012 *Journal of Materials Engineering and Performance* **21** 1539–1551
[2] He X, Zhao D, Sun X and Zhu B 2017 *Journal of Pressure Vessel Technology* **139** 041601–041601–9
[3] Han M, Liu Y, Wu D, Zhao X and Tan H 2017 *International Journal of Heat and Mass Transfer* **111** 1–16
[4] Benjamin T B and Ellis A T 1966 *Philosophical Transactions of the Royal Society of London* **260** 221–240
[5] Cui P, Zhang A M, Wang S P and Wang Q X 2013 *Applied Ocean Research* **41** 65–75
[6] Li X, Jia L, Dang C, An Z and Huang Q 2018 *Experimental Thermal and Fluid Science* **91** 230–244
[7] Xue T, Qu L and Wu B 2014 *IEEE Transactions on Instrumentation and Measurement* **63** 1639–1647
[8] Bauer D, Chaves H and Arcoumanis C 2012 *Measurement Science and Technology* **23** 055302
[9] Zhao G, Zhao H, Shu H and Zhao D 2010 *Advances in Natural Science* 17–26
[10] Ren S, He K, Girshick R and Sun J *Advances in neural information processing systems* pp 91–99